Validation Report for "Cloud Products" (CMa-PGE01, CT-PGE02 & CTTH-PGE03 v1.4)

SAF/NWC/CDOP/MFL/SCI/VR/02, Issue 1, Rev. 4

7 November 2007

Applicable to SAFNWC/MSG version 2008

Prepared by Météo-France / Centre de Météorologie Spatiale

REPORT SIGNATURE TABLE

Function	Name	Signature	Date
Prepared by	MF/DP/CMS		
Reviewed by	MF/DP/CMS		
Authorised by	L. F. López Cotín SAFNWC Project Manager		*7 November 2007*

DOCUMENT CHANGE RECORD

Version	Date	Pages	CHANGE(S)
1.4	7 November 2007	30	

Table of contents

List of Tables and Figures

1. INTRODUCTION

1.1 SCOPE OF THE DOCUMENT

An extensive validation of PGE01-02-03 v1.2 has been performed in 2005 and documented in a validation report ([AD. 1]).

The algorithm has remained unchanged in v1.3 (included in the release2007 of the SAFNWC/MSG SW package) and therefore no new validation report was produced.

The algorithm in v1.4 (included in the release2008 of the SAFNWC/MSG SW package) has also remained unchanged. But Eumetsat plans a change in 2008 of the currently disseminated SEVIRI IR "spectral radiances" into "effective radiance" (see [AD. 3]), leading to changes in brightness temperature that can exceed 1K for some channels. The release2008 of the SAFNWC/MSG SW package systematically checks the status of the SEVIRI radiances input by the users and if necessary transform them in "effective radiances". Therefore our PGE01-02-03 have been slightly tuned to account for the change in brightness temperatures induced by the change in the radiance definition.

In the rest of the document:

- **v1.4** refers to the version v1.4 applied to "effective radiances" which is validated in this document.
- **v1.3** refers to the previous version v1.3 applied to "spectral radiances" which was validated in 2005 ([AD. 1]).

This document provides the accuracies reaches by CMa, CT and CTTH v1.4. These accuracies are compared to the target accuracies for the CDOP period listed in [AD. 2]. They are also compared to the accuracies reached by CMa, CT and CTTH v1.3.

1.2 SOFTWARE VERSION IDENTIFICATION

The validation results presented in this document apply to the algorithms implemented in the PGE01-02-03 version 1.4 included in the release2008 of the SAFNWC/MSG SW package using "effective radiances".

1.3 DEFINITIONS, ACRONYMS AND ABBREVIATIONS

ARPEGE	French weather forecast model
BUFR	European Centre for Medium range Weather Forecast
CDOP	Continuous Development and Operational Phase
CMa	Cloud Mask (also PGE01)
CMS	Centre de Météorologie Spatiale (Météo-France, satellite reception and processing centre in Lannion)
CT	Cloud Type
CTTH	Cloud Top Temperature and Height
IR	Infrared
MSG	Meteosat Second Generation
SAFNWC	Satellite Application Facility for support to NoWcasting
SEVIRI	Spinning Enhanced Visible & Infrared Imager
SIRTA	Site Instrumental de Télédetection Atmosphérique (located near Paris)
SYNOP	Synoptic observation
SW	SoftWare

1.4 REFERENCES

1.4.1 Applicable Documents

Reference	Title	Code	Vers	Date
[AD. 1]	Validation report for the PGE01-02-03 (v1.2) (Cloud Products) of the SAFNWC/MSG	SAF/NWC/IOP/MFL/SCI/VAL/01	1.2	17/01/07
[AD. 2]	NWCSAF Product Requirements Document	SAF/NWC/CDOP/INM/MGT/PRD	0.1	30/08/07
[AD. 3]	Change to the MSG Level1.5 Image product Radiance Definition	EUM/STG-OPS/21/07/DOC/04		20/02/07

Table 1 List of Applicable Documents

1.4.2 Reference Documents

Reference	Title	Code	Vers	Date
[RD.1]				
[RD.2]				

Table 2 List of Referenced Documents

2. CMA VALIDATION

2.1 OVERVIEW

2.1.1 General objectives of the validation

The main objective of this section is to document CMa accuracies and compare them to the target accuracies listed in [AD. 2]. Additionally, CMa accuracies are compared to those obtained with the previous version.

2.1.2 Methodology outline

The following validation of the CMa product is performed:

- ✓ The CMa cloud mask (v1.4) is validated for all seasons over European areas using SYNOP data. The POD (Probability Of Detection) is computed and is compared to the target value for the CDOP period ([AD. 2]) and to the value reached with the previous version (v1.3).
- ✓ The CMa dust detection (v1.4) is validated from interactively selected targets over seas and Africa for solar elevation larger than 20 degrees. The POD (Probability Of Detection) is computed and is compared to the target value for the CDOP period ([AD. 2]) and to the value reached with previous version (v1.3).

In all these validation studies, CMa is retrieved using NWP fields forecast by the French model ARPEGE four times per day (0h, 6h, 12h and 18h) at a 1.5 degree horizontal resolution.

2.2 CMA CLOUD MASK: COMPARISON WITH SURFACE OBSERVATION (SYNOP)

The quantitative comparison of the CMa cloud mask with surface synoptic observations is made possible thanks to the use of the coincident satellite targets and SYNOP data gathered from 1st November 2003 up to 28th February 2005 from terrestrial stations over Europe and North Africa, (only manned stations (the selected station dataset (SSD) subset), shown in Figure 4, are retained in the statistics). The satellite part of the dataset (described in Annex 2) allows the reprocessing of different version of CMa and also allows the simulation of "effective radiances" from the stored "spectral radiances".

From the SYNOP data set, ground-based total cloud cover (N) and partial cloud cover from low, medium and high clouds are available. Satellite cloud coverage is estimated from CMa applied to the pixels of the satellite targets. To simulate the surface observations from the satellite pixels, no attempt is made to take into account the complexity of the observation, and the 25 pixels inside the satellite data target are used for the evaluation. The total cloudiness over SYNOP station is simply simulated from CMa results over the 5x5 target centred on the station by counting each pixel detected as cloud contaminated as 100% covered.

The CMa cloud mask validation examines only cases that show disagreement with SYNOP cloud cover, i.e. when CMa misses clouds reported almost overcast by the ground observer and when CMa detects clouds where SYNOP report no or insignificant cloud cover. For this purpose we build up two-by-two contingency tables counting "cloudy" and "clear" events. An observation is cloudy if N from SYNOP is strictly more than 5 octas, clear if N is strictly less than 3 octas. A detection is cloudy if more than 16/25 pixels are flagged cloud contaminated, clear if less than 8/25 are clear. Consequently all events with N=3,4,5 and equivalent CMa cloud covers expressed in octas are not taken into account in these statistics. This study relies on analysis of contingency tables and comparison of statistical scores.

	Cloud detected	Clear detected
Cloud observed	h	m
Clear observed	fa	cr

Table 3 Contingency table conventions for CMa validation (h for hits, m for misses, fa for false alarm and cr for correct rejection)

The following statistical indicators derived from the contingency tables (see Table 3) are computed:

- PC= [(h+cr)/(H+m+fa+cr)], is the percentage of correct detections (PC)

Two following statistical indicator stratified by observation are computed (the POD (Probability Of Detection) should be as high as possible and the FAR (False Alarm Rate) as low as possible):

- POD=[h/(h+m)], is the rate of correctly detected cloud observations, i.e. targets classified as cloudy and observed cloudy.
- FAR=[fa/(fa+cr)], is the rate of missed clear observations or false flagging of clouds, i.e. the targets classified as cloudy but observed clear (it expresses cloud overdetection errors)

Contingency tables and statistical scores have been computed by gathering all illumination conditions (day, night, twilight) for all selected SYNOP station (Figure 4).

The results for CMA v1.4 and v1.3 are displayed in the following Table 4.

	PC (%)	POD(%)	FAR(%)
CMa v1.4	94.77	95.90	7.65
CMa v1.3	94.74	95.93	7.82

Table 4 CMa performance in the detection of fully cloudy and cloud-free events estimated from collocated surface and MSG-1/SEVIRI observations from 01/11/2003 to 28/02/2005 (539000 matchups)

The POD reached by the CMa (v1.4) cloud detection is 95.90% while the target POD for the CDOP period is 95.0% (see [AD. 2]). It can also be seen that the POD reached by CMa cloud detection v1.4 (95.90%) is very similar to the one obtained from v1.3 (95.93%).

2.3 CMA DUST FLAG VALIDATION

The database available at CMS to quantify the CMa dust flag is the Interactive Target Database (see Annex 1) which gathers about 3800 targets corresponding to dust events located over Africa and adjacent seas (Figure 1 shows their location).

The satellite part of the dataset (described in Annex 2) allows the reprocessing of different version of CMa and also allows the simulation of "effective radiances" from the stored "spectral radiances".

Statistical scores are indicators of how much the automated CMa dust flag agrees with the interactively manned targets types. Note that no attempt to quantify the thin dust clouds detection over Europe has been performed as all the targets corresponds to dust storms over Africa or adjacent seas.

The following statistical scores stratified by observation are computed from contingency tables built from this database (see Table 5 for conventions; "dust detected" corresponds to more than half the pixels of the target flagged as dust by CMa; "no dust detected" corresponds to less than half the pixels of the target flagged as dust by CMa) :

- POD=[h/(h+m)], is the rate of correctly detected dust observations, i.e. targets classified as dust and observed dust (it expresses the dust correct detection).
- FAR=[fa/(fa+cr)], is the rate of false flagging of dust, i.e. the targets classified as dust but observed without dust (it expresses dust overdetection errors)

	Dust detected	No dust Detected
Dust observed	h	m
No dust observed	fa	cr

Table 5 Contingency table conventions (h for hits, m for misses, fa for false alarm and cr for correct rejection)

The POD (Probability Of Detection) should be as high as possible and the FAR (False Alarm Rate) as low as possible.

Database is stratified according to land and sea and is limited to solar elevation larger than 20 degrees. Results are sum up in Table 6 and Table 7.

	Contingency table (over sea)		FAR (%)	POD (%)
CMa/dust v1.4	504	807	0.9	38.5
	23	2654		
CMa/dust v1.3	505	806	0.9	38.5
	23	2654		

Table 6 Dust flag performance over sea estimated from the Interactive Target Database

	Contingency table (over land)		FAR (%)	POD (%)
CMa/dust v1.4	1294	918	0.6	58.5
	20	3131		
CMa/dust v1.3	1338	874	0.8	60.5
	26	3125		

Table 7 Dust flag performance over land estimated from the Interactive Target Database

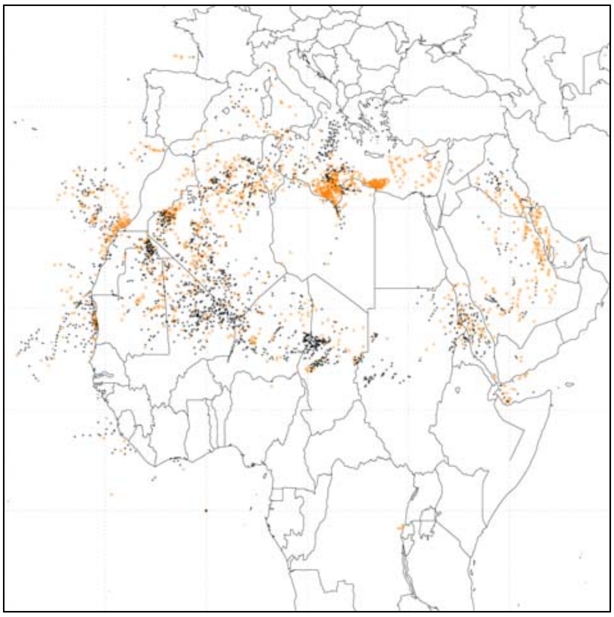

Figure 1 Localisation of the interactive targets corresponding to dust events. Black symbol and orange diamond correspond respectively to detected and non detected by the CMa dust flag.

The POD reached by the CMa (v1.4) dust detection is 58.5% over land and 38.5% over sea while the target POD for the CDOP period is 50% (see [AD. 2]).

2.4 ASSESSMENT OF ALGORITHM QUALITY

The CMa v1.4 cloud detection reaches the target accuracy for the CDOP period: the v1.4 POD (95.90%) is larger than the target POD (95.0%) for the CDOP period.

The CMa v1.4 dust detection reaches the target accuracy for the CDOP period over Africa: the v1.4 POD 58.5% is larger than the target POD (50%) for the CDOP period. But this is not the case over sea, where the v1.4 POD (38.5%) is lower than the target POD (50%) for the CDOP period. This is normal as the algorithm v1.4 does not yet include the planned CDOP improvement of dust detection over sea.

The accuracies of the CMa cloud detection and dust detection reached in v1.4 and in v1.3 are very similar, meaning that the change of the radiance definition planned in 2008 will have no noticeable impact on CMa products.

3. CT VALIDATION

3.1 OVERVIEW

3.1.1 General objectives of the validation

The main objective of this validation report is to document CT accuracies and compare them to the target accuracies listed in [AD. 2]. Additionally, CT accuracies are compared to those obtained with the previous version.

3.1.2 Methodology outline

The following validation of the CT product is performed:

- ✓ The CT cloud type (v1.4) is validated for all seasons over European areas and adjacent seas using the Interactive Target database. The "User Accuracy" is computed and is compared to the target value for the CDOP period ([AD. 2]) and to the value reached with previous version (v1.3).

In all these validation studies, CT is retrieved using NWP fields forecast by the French model ARPEGE four times per day (0h, 6h, 12h and 18h) at a 1.5 degree horizontal resolution.

3.2 COMPARISON WITH INTERACTIVE TARGET DATABASE

The Interactive Target Database (see Annex 1) allows the comparison of the CT cloud types and the cloud class manually labelled from SEVIRI imagery. This comparison is an indicator of the CT algorithm's quality but also of the separability of the cloud classes, and a way to understand how the CT algorithm manages classes. Although the interactive target have been gathered over the MSG full disk, the validation is restricted to all targets in the MSG full disk at a latitude larger than 20degreN (which roughly corresponds European area and adjacent seas). The satellite part of the dataset (described in Annex 2) allows the reprocessing of different version of CT and also allows the simulation of "effective radiances" from the stored "spectral radiances".

The CT and the manually labelled cloud classes are first gathered into the main classes described in Table 8 before being compared. There is an agreement if the most probable CT main class (i.e. the most frequent main class among the 9 central pixels) is identical to the observer main class. As clear and cloud confusions have been analysed in CMa validation section, the database is limited to cases identified as cloudy by the observer and CT.

Contingency tables and statistical scores (user's accuracy (probability of a pixel classified into a category on a picture to really belong to that category)) are then computed. They are associated with changes illumination (day, night, twilight).

Main Classes name	Target type	CT type
Sea	Open sea, Sea with haze, Sea with shadow, Sea with sunglint	Sea not contaminated by clouds, aerosol or ice/snow
Land	Land, land with haze, land with shadow,	Land not contaminated by clouds, aerosol or snow
Ice	Ice, ice with shadow	Sea contaminated by ice/snow
Snow	Snow, snow with shadow	Land contaminated by snow
Low clouds	Fog, stratus, small cumulus over land, small cumulus over sea Stratocumulus, stratocumulus with shadow	Very low clouds Low clouds

Mid-level clouds	Altocumulus, Altostratus, cumulus congestus over land and sea	Medium clouds
Semitransparent	Thin cirrus above stratus or stratocumulus or cumulus Thin cirrus over sea, thin cirrus over land, thin cirrus over snow, thin cirrus over ice Cirrostratus	Cirrus above lower clouds Thin cirrus Mean and thick cirrus
High clouds	Cirrostratus over Altocumulus or Altostratus. Thin cirrus over Ac As Isolated or merged Cb	High opaque clouds Very high opaque clouds

Table 8 Equivalence between manually labelled targets and CT types

CT v1.4	Low clouds	Mid-level clouds	Semitransparent	High clouds
All illumination	93.40 %	36.66 %	90.95 %	79.43 %
Daytime	90.89 %	47.87 %	94.08%	78.40 %
Nightime	94.82 %	28.86 %	85.12 %	80.15 %
Twilight	96.34 %	25.49 %	82.14 %	84.62 %

Table 9 Users accuracy for each main cloud classes estimated from the Interactive Target database stratified by illumination. For v1.4 applied to "effective radiances".

CT v1.3	Low clouds	Mid-level clouds	Semitransparent	High clouds
All illumination	93.30 %	36.82 %	90.79 %	79.96 %
Daytime	90.76 %	48.00 %	93.77 %	78.95 %
Nightime	94.82 %	29.08 %	85.25 %	80.77 %
Twilight	96.02 %	25.49 %	82.76 %	84.62 %

Table 10 Users accuracy for each main cloud classes estimated from the Interactive Target database stratified by illumination. For v1.3 applied to "spectral radiances".

Table 9 Shows that the users accuracies obtained by CT v1.4 for low clouds (93.40%), high clouds (79.43%) and semi-transparent clouds (90.95%) are above the target user accuracy for the CDOP period which was 70% ([AD. 2]).

3.3 Assessment of algorithm quality

The CT v1.4 cloud type reaches the target accuracy for the CDOP period: the user accuracies obtained by CT v1.4 for low clouds (93.40%), high clouds (79.43%) and semi-transparent clouds (90.95%) are far above the minimum value for the CDOP period which is 70%

The accuracies of the CT cloud type reached by CT v1.4 and by CT v1.3 are very similar, meaning that the change of the radiance definition planned in 2008 will have no noticeable impact on CT products, as illustrated in Figure 2.

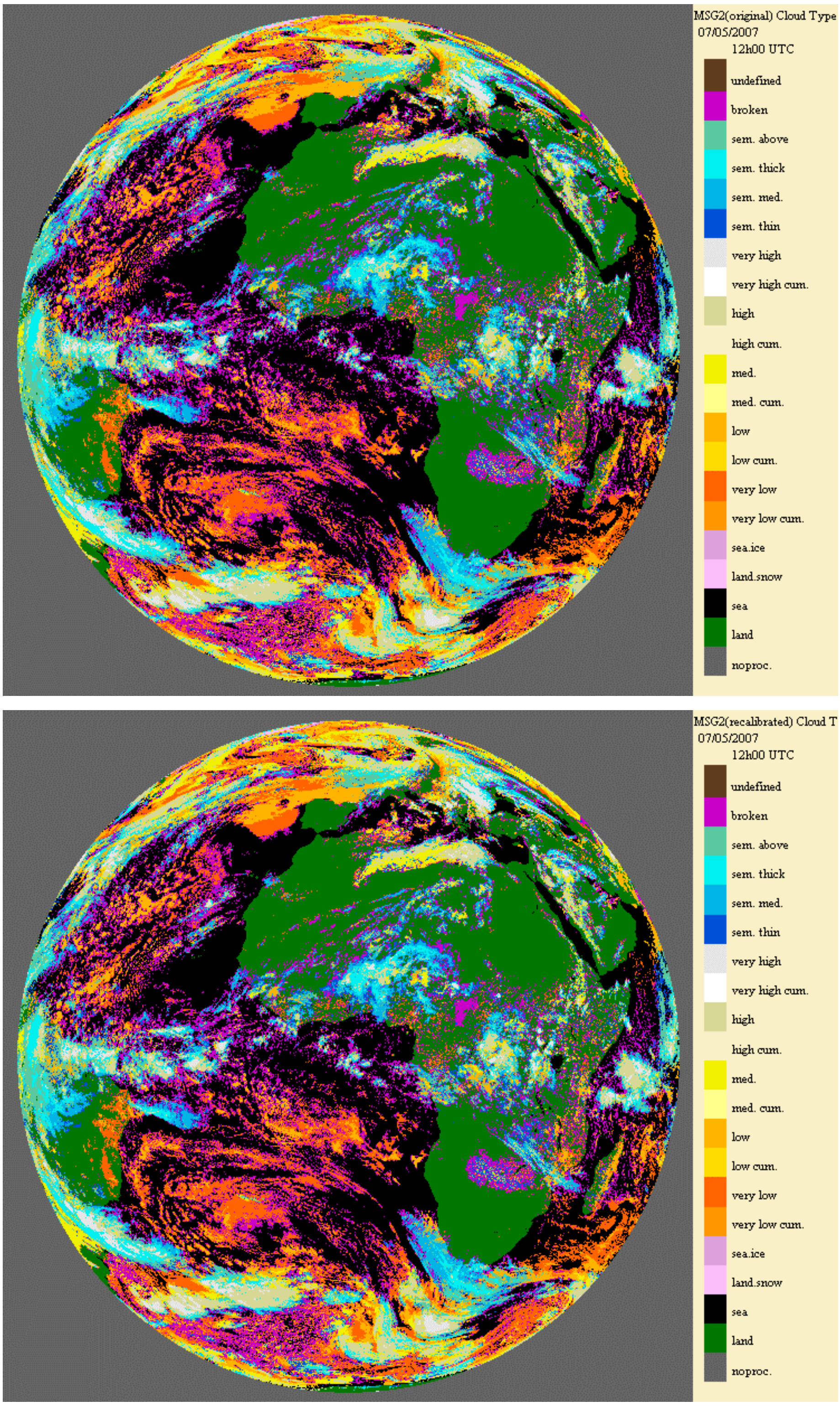

Figure 2 Example of CT cloud type processed with v1.3 applied to spectral radiances (top figure) and v1.4 applied to effective radiances (bottom figure)

4. CTTH VALIDATION

4.1 OVERVIEW

4.1.1 General objectives of the validation

The main objective of this validation report is to document CTTH accuracies and compare them to the target accuracies listed in [AD. 2]. Additionally, CTTH accuracies are compared to those obtained with the previous version.

4.1.2 Methodology outline

The following validation of the CTTH product is performed:

- ✓ The CTTH cloud height (v1.4) is validated with one year (September 2003-October 2004) of measurements from the ground-based lidar and radar from the SIRTA instrumented site (near Paris). The biases and standard deviation are computed and compared to the target values for the CDOP period ([AD. 2]) and to the ones obtained with previous version (v1.3).

In all these comparisons, CTTH is retrieved using NWP fields forecast by the French model ARPEGE four times per day (0h, 6h, 12h and 18h) at a 1.5 degree horizontal resolution. Temperature and humidity are available on twenty pressure levels (10, 20, 30, 50, 70, 100, 150, 200, 250, 300, 400, 500, 600, 700, 800, 850, 900, 925, 950, 1000).

4.2 VALIDATION OF CTTH WITH GROUND-BASED LIDAR AND RADAR

The validation of the CTTH (Cloud Top height) quality with measurements from ground-based lidar and radar located near Paris is performed from a dataset gathering ground-based radar and lidar measurements (described in Annex 4) and satellite data (described in Annex 2, allowing the reprocessing of CTTH and the simulation of effective radiance from the stored spectral radiances) and covering the period September 2003-October 2004.

The ground-based measurements used in this study are provided by SIRTA (Site Instrumental de Recherche par Télédétection Atmosphérique), an atmospheric observatory for cloud and aerosol research operated by the Institut Pierre Simon Laplace (IPSL). The SIRTA observatory is located on the campus of Ecole Polytechnique, Palaiseau, France. SIRTA is composed of an ensemble of state-of-the-art active and passive remote sensing instruments, including radars, lidars and radiometers. A detailed description of the radar and lidar measurements is given in Annex 4.

The following procedure is applied to SEVIRI, lidar and radar measurements to gather the validation dataset:

- Because of the difference in spatial resolution between the ground-based and satellite sensors, the approach is to perform a temporal average of the ground-based data over a period of time and compare with spatially averaged SEVIRI cloud top height retrievals. In the present work, the cloud properties derived from observations at SIRTA are averaged temporally over 30 minutes and the SEVIRI cloud properties are averaged spatially over 5x3 pixels.
- Because of inherent discrepancies in ground and spatial observational scales, focusing the comparison on homogeneous situations will minimize scale-induced variability. Hence, the comparison is restricted to the SEVIRI scenes showing a large homogenous cloud

coverage (low/middle or high/semi-transparent cloud fractions must be larger than 80 % within an area of 11x7 pixels and 50% within an area of 5x3 pixels).

- When more than one cloud layer is detected by the radar or the lidar, the SEVIRI CTH is systematically compared with the nearest layer of ground-based instrument dataset.
- Suspect cases have been manually analysed by displaying the full SEVIRI images and the full lidar and radar measurements. They often corresponds to multilayer clouds where the upper semi-transparent cloud layer was not automatically detected from the radar/lidar measurements. These cases have been removed from the study. There certainly still remains such cases, therefore part of the comparison errors certainly comes from the ground-based radar/lidar measurements themselves.

Validation results are presented for opaque clouds and semi-transparent clouds (using either intercept or radiance ratioing methods).

4.2.1 Opaque clouds

In this section, we analyse SEVIRI CTH retrieval for opaque clouds. Although lidar is the best instrument to measure cloud boundaries, lidar measurements are strongly attenuated by most of opaque clouds and therefore, the signal often does not reach the cloud top. Radar measurements are therefore needed to measure the top height of opaque clouds. For opaque clouds, we therefore use RALI measurements (synergie of radar and lidar, described in Annex 4) during radar time acquisition (operational mode 0).

	Bias (km)	Standard deviation (km)	Number of cases
CTTH v1.4 (low clouds)	0.42	1.04	1137
CTTH v1.4 (high or mid-level clouds)	-0.36	1.17	1030
CTTH v1.3 (low clouds)	0.32	1.03	1143
CTTH v1.3 (high or mid-level clouds)	-0.40	1.17	1030

Table 11 Low opaque and mid-level/high opaque clouds statistical scores for (CTH_SEVIRI-CTH_RALI) Negative bias values correspond to SEVIRI CTH underestimation.

	Bias (km)	Standard deviation (km)	Number of cases
CTTH v1.4	0.05	1.17	2167
CTTH v1.3	-0.02	1.15	2173

Table 12 Opaque clouds statistical scores for (CTH_SEVIRI-CTH_RALI) Negative bias values correspond to SEVIRI CTH underestimation.

The opaque clouds bias and standard deviation values obtained with CTTH v1.4 (0.05km and 1.17km) are lower that the target values for the CDOP period (0.5km and 1.5km).

The results obtained with CTTH v1.3 and v1.4 are very similar.

4.2.2 Semi-transparent clouds

Two types of method can be applied to retrieve the cloud top pressure or height of semi-transparent clouds: the intercept method and the radiance ratioing technique which is only applied to the thickest semi-transparent clouds. Figure 3 illustrates the typical range of effective emissivities for clouds having their top pressure retrieved by the intercept or the radiance ratioing technique.

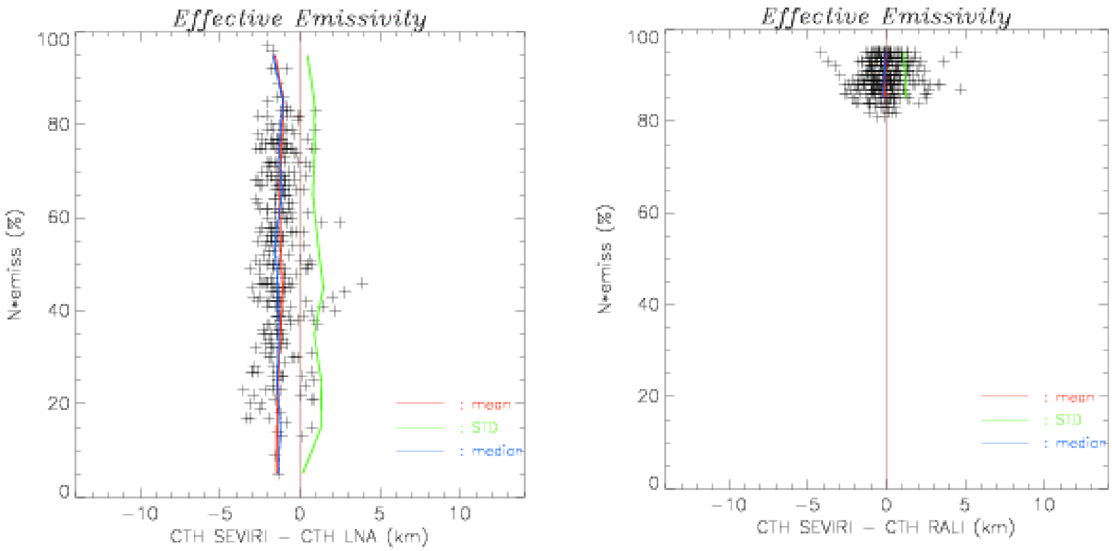

*Figure 3 Illustration of the range of effective emissivity (N*emiss in % in the vertical scale) for semi-transparent clouds having their cloud top pressure retrieved by the intercept method (left) and radiance ratioing technique (right).*

The accuracy of each method will be evaluated separately, the intercept method corresponding to the thinnest semi-transparent clouds and the radiance ratioing being applied to the thickest semi-transparent clouds.

4.2.2.1 Semi-transparent clouds with intercept method

In general, radar instruments are able to detect most cloud, except thin cirrus and thin strato-cumulus, however the lidar is ideally suited to this task. For the study of semi-transparent cloud, we only used lidar measurements to perform the validation. In case of the presence of a low cloud layer with a high optical depth, a thin cirrus could be not detected by the lidar. Because the lidar is subject to attenuation, we imposed that the mean range of LNA instrument during the 30 minutes time period was higher than 8 km. Most of multi-layer cloudy scene are therefore excluded for this study.

	Bias (km)	Standard deviation (km)	Number of cases
CTTH v1.4	-1.09	1.09	316
CTTH v1.3	-1.08	1.09	314

Table 13 Statistical scores for (CTH_SEVIRI-CTH_LNA) when the intercept method is used. Negative bias values correspond to SEVIRI CTH underestimation.

The semi-transparent clouds bias and standard deviation values obtained with CTTH (intercept method) v1.4 (1.09km and 1.09km respectively) are lower that the target values for the CDOP period (1.5km).

The results obtained with CTTH v1.3 and v1.4 are very similar.

4.2.2.2 Semi-transparent clouds with radiance ratioing method

The radiance ratioing method is applied to semi-transparent clouds whose effective emissivity is higher than .80 (nearly opaque cloud) and is giving results at pixel scale. This method is only applied to semi-transparent clouds if no reliable retrieved cloud top pressure is found using intercept method. Clouds analysed in this section are much thicker than in case the cloud top is retrieved by intercept method. In order to increase the number of available cases, we used RALI ground-based measurements when at least one of the two instruments operated (optional mode 3).

	Bias (km)	Standard deviation (km)	Number of cases
CTTH v1.4	-0.09	1.02	223
CTTH v1.3	-0.09	1.12	210

Table 14 Statistical scores for (CTH_SEVIRI-CTH_RALI) when in the radiance ratioing method is used. Negative bias values correspond to SEVIRI CTH underestimation.

The semi-transparent clouds bias and standard deviation values obtained with CTTH (radiance ratioing technique) v1.4 (0.09km and 1.02km) are lower that the target values for the CDOP period (1.5km).

It can be noticed that the bias observed with v1.3 and v1.4 are very much the same but with a slightly lower standard deviation for v1.4 (1.02km instead 1.12km).

4.3 ASSESSMENT OF ALGORITHM QUALITY

The CTTH v1.4 reaches the target accuracy for both opaque clouds and semi-transparent clouds. For opaque clouds, bias and standard deviation values obtained with CTTH v1.4 (0.05km and 1.17km) are much lower that the target values for the CDOP period (0.5km and 1.5km). Concerning semi-transparent clouds, bias and standard deviation values obtained with CTTH v1.4 are lower that the target values for the CDOP period, either when the intercept method is used [v1.4 bias (std): 1.09km (1.09km) to be compared to CDOP target bias (std):1.5km (1.5km)] or for the thickest semi-transparent clouds using the radiance ratioing technique [v1.4 bias (std): 0.09km (1.02km) to be compared to CDOP target bias (std):1.5km (1.5km)].

ANNEX: TEST AND VALIDATION DATASET

ANNEX 1 INTERACTIVE TARGET DATABASE

An interactive tool, based on the use of the commercial image processing software WAVE, has been used by experienced operators for the extraction of visually identified satellite targets in SEVIRI images (area : full disk). The result of this work is a dedicated database for spectral signature studies that we call the Interactive Target Database. Such a database has been already been gathered from GOES and MODIS during prototyping activities. The interactive procedure allows :

- the display of various channels combination full resolution in satellite projection,
- the zoom of an area
- the choice of small square targets (configurable size, by default: 5*5 SEVIRI IR pixels)
- the labelling of the targets through a menu

The Interactive Target Database gathers the following information (detailed below) for each satellite target:

- the label given by the operator to the target (list displayed in Table 15 below),
- the full satellite information in the square targets together with satellite & solar angles and time information,
- the collocated and nearest in time meteorological information extracted from ARPEGE forecast fields,
- collocated atlas values.

Open sea	Sea with shadow	Sea with sand aerosols	Sea with ash
Sea with haze	Sea with sunglint	Sea with volcanic plume	
Land	Land with shadow	Land with sand aerosol	Land with ash
Land with Haze	Land with volcanic plume	Ice	Ice with shadow
Snow	Snow with shadow	Unclassified (cloudy or cloudfree)	Cloudy (unknown)
fog	stratus	Stratocumulus	shadow over low clouds
small cumulus over sea	Cumulus congestus over sea	small cumulus over land	Cumulus congestus over land
Cumulonimbus	Extensive cumulonimbus	Thin cirrus over sea	Thin Cirrus over ice
Thin cirrus over land	Thin cirrus over snow	Thin cirrus over St/Sc	Thin cirrus over Cu
Thin cirrus over Ac/As	Altocumulus/Altrostratus	Altocumulus	Cirrostratus
Cirrostratus over Ac/As			

Table 15 List of cloud & earth types available in the Interactive Target Database

ANNEX 2 FORMAT FOR SEVIRI SATELLITE TARGET

Satellite targets are gathered, either manually with the Interactive Target Database, either automatically around synoptic meteorological stations or around the SIRTA site.

Each satellite target window will be have a configurable size, the default size being 5 columns by 5 rows (3km IR pixel) (33*33 for the SIRTA site).

The satellite targets contains the following information that allows the reprocessing of PGE01-02-03 (for example to validate different versions):

<u>Full satellite information in the square targets, together with satellite & solar angles and time information :</u>

type	a*2 target type (in for interactive)
observer	a*10 user name of the person who has analysed the target
lat	i*4 latitude of the centre of the target (1000th of degrees)
lon	i*4 longitude of the centre of the target (1000th of degrees)
date	i*4 julian day (count from 00h, 1 Jan 1950)
hour	i*4 UTC time of day in milliseconds
idsat	i*4 satellite identification (1=MSG1, 2=MSG2, 3=MSG3)
nbp	i*2 number of columns expressed in 3km IR coordinates
nbl	i*2 number of rows expressed in 3km IR coordinates
nbc	i*2 number of channels (7,10 or 11, according to day/night consideration and HRV availability)
valcan_VIS06	I*2 indicator of VIS0.6 availability
valcan_VIS08	I*2 indicator of VIS0.8 availability
valcan_IR16	I*2 indicator of IR1.6 availability
valcan_IR38	i*2 indicator of IR3.8 availability [-1 =not in the file
valcan_WV62	i*2 indicator of WV62 availability [0 =is missingt
valcan_WV73	i*2 indicator of WV73 availability [>0 =mean value in the
valcan_IR87	i*2 indicator of IR87 availability [target(unit: 1/100 % or 1/100 K)]
valcan_IR97	i*2 indicator of IR97 availability
valcan_IR108	i*2 indicator of IR108 channel availability
valcan_IR120	i*2 indicator of IR120 channel availability
valcan_IR134	i*2 indicator of IR134 channel availability
valcan_HRV	I*2 indicator of HRV availability
canal VIS06	x i*2 window from VIS06 (x = nbp*nbl) in 1/100 %
canal VIS08	x i*2 window from VIS08 (x = nbp*nbl) in 1/100 %
canal IR6	x i*2 window from IR16 (x = nbp*nbl) in 1/100 %
canal IR38	x i*2 window from IR38 (x = nbp*nbl) in 1/100 K
canal WV62	x i*2 window from WV62 (x = nbp*nbl) in 1/100 K
canal WV73	x i*2 window from WV73 (x = nbp*nbl) in 1/100 K
canal IR87	x i*2 window from IR87 (x = nbp*nbl) in 1/100 K
canal IR97	x i*2 window from IR97 (x = nbp*nbl) in 1/100 K
canal IR108	x i*2 window from IR108 (x = nbp*nbl) in 1/100 K
canal IR120	x i*2 window from IR120 (x = nbp*nbl) in 1/100 K
canal IR134	x i*2 window from IR134 (x = nbp*nbl) in 1/100 K
canal HRV	x i*2 window from HRV (x = 3*nbp*3*nbl) in 1/100 %
solzen	i*2 solar zenith angle (100th of degrees)
satzen	i*2 satellite zenith angle (100th of degrees)
daz	i*2 local azimuth angle (100th of degrees)s
typ_cloud	i*2 target code (given by the observer , or –9999 if automatically fed)

Full CMa/CT/CTTH results in the square targets:

CMa main categories	x i*1 window from CMa main categories (x = nbp*nbl)
CMa tests	x i*2 window from CMa tests (x = nbp*nbl)
CMa quality flag	x i*2 window from CMa quality flag (x = nbp*nbl
CT main categories	x i*1 window from CT main categories (x = nbp*nbl)
CT quality flag	x i*2 window from CT quality flag (x = nbp*nbl
CTTH top pressure	x i*1 window from CTTH top pressure (x = nbp*nbl)
CTTH top temperature	x i*1 window from CTTH top temperature (x = nbp*nbl)
CTTH top height	x i*1 window from CTTH top height (x = nbp*nbl)
CTTH cloudiness	x i*1 window from CTTH cloudiness (x = nbp*nbl)
CTTH quality flag	x i*1 window from CTTH quality flag (x = nbp*nbl)

Collocated atlas values and climatological values :

land/sea	x i*1 land/sea atlas (space=0, sea=2, land=3), (x = nbp*nbl)
land/sea/coast	x i*1 land/sea/coast atlas (space=0, coast=1,sea=2, land=3), (x = nbp*nbl)
height	x i*2 height atlas value (in meters), (x = nbp*nbl)
stt	x i*2 sst climatological value (in 1/100 K), (x = nbp*nbl)
albedo	x i*2 visible reflectance climatological value (in 1/100 %), (x = nbp*nbl)
h2o	i*2 climatological integrated water vapor content (in 1/100 kg/m2)
T1000	i*2 climatological air temperature at 1000hPa (in 1/100 K)
T850	i*2 climatological air temperature at 850hPa (in 1/100 K)
T700	i*2 climatological air temperature at 700hPa (in 1/100 K)
T500	i*2 climatological air temperature at 500hPa (in 1/100 K)

Collocated and nearest in time meteorological information extracted from ARPEGE forecast fields (temperature & humidity vertical profile) [missing values : -9999] :

Modele a*7 name of modele (ARPEGE or ECMWF…)

Two set of forecast NWP fields are available (nearest in time before and after SEVIRI image):

date	i*4 julian day of forecast day (count from 00h, 1 Jan 1950)
res	i*4 hour of forecast
ech	i*4 forecast term (in hour)
HeightNWP	I*4 height of NWP grid (in meters)
psol	i*4 ground pressure (1/100 hPa)
tsol	i*4 ground temperature (1/100 K)
t2m	i*4 2m air temperature (1/100 K)
hu2m	i*4 2m air relative humidity (1/100 %)
nbniv	I*4 number of pressure levels on the vertical
pniv	20 i*4 nbniv pressure level (in hPa)
tniv	20 i*4 temperature at nbniv pressure levels (1/100 K)
huniv	20 i*4 relative humidity at nbniv pressure levels (1/100 %)
ptropo	i*4 pressure at tropopause level (1/100 hPa)
ttropo	i*4 temperature at tropopause level (1/100 K)
W	i*4 integrated water vapor content (in 1/100 kg/m2)

Spare values :

spare 30 i*4 spare data (not used)

ANNEX 3 SURFACE OBSERVATIONS (SYNOP)

The data used are the routine weather observations, coded by the observers into the WMO synoptic code, gathered at Toulouse and made available to users through a METEO-FRANCE data base. From this data base we extract all the synoptic reports (coded in BUFR) from a list of 535 selected land stations, over the European and Northern African area. These stations have been selected to cover European region. The SYNOP network status is permanently evolving because several nations are replacing human cloud cover observations by automatic systems delivering cloud covers. For this reason we decided to keep from the initial database only the SYNOP whose $i_x < 4$ (in $i_R i_x hVV$ group of section 1 of SYNOP, coded according to table code 1860 of the WMO manual on codes) because they are assumed to be manned station. Another indicator of human observation is the anomaly at N=1 or N=7 in the N distribution (N1N7) of a station, as according to WMO standard for reporting cloud cover, a very small cloud in the sky leads human observer to code 1 octa, rather than 0, and, in a similar way, a small patch of clear sky gives rise 7 rather than 8 octas. We analyse these statistics by station and retain only those for which N1N7 anomaly is observed. We are aware that this distribution may change with time and that automatic observations may still enter our statistics. Our final set contains 302 stations, their spatial distribution is displayed on right part of Figure 4. This set is the basis retained for our statistics when we deal with "selected stations dataset" (SSD), otherwise we specify "no selection among stations" (NSASD). It is obvious that some countries are not covered by this geographical distribution, but considering the one-year duration and the dispersion of the stations, it should not hamper the study.

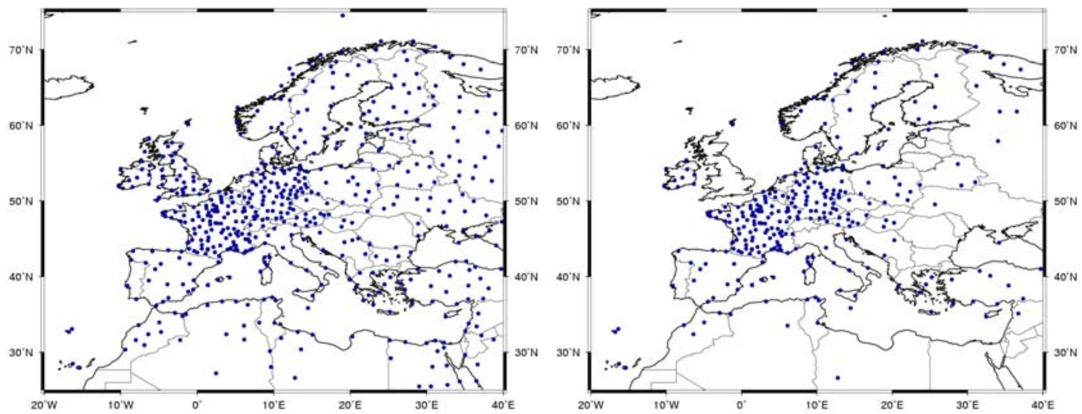

Figure 4 Geographical distribution of SYNOP stations, gathered from November, 1st 2004 till February, 28 th 2005; left initial set (NSASD set); right 302 selected stations(SSD set)

The database has been built as soon as MSG data were routinely available at CMS through EUMETCast diffusion with a stable geo-location and radiometric quality. We have used information from November 2003 till February 2005, with an interruption in January 2004 during the satellite positioning towards -3.4W. The SYNOP are selected with 3 hour intervals and gathered with MSG/SEVIRI information coming from the slot starting 15 minutes before.

To avoid cases where solar intrusion in IR 3.9 µm at night-time is significant, we also rejected from SSD selection all the matchups presenting a mean reflectance in SEVIRI VIS 0.6 µm greater than .9% with a sun zenithal angle greater than 93 degrees. Finally from a NSASD containing 1138432 samples, we get a SSD with 708793 usable sorted matchups. This dataset can be stratified according to station latitude. The Nordic subset (16%) contains stations with latitude higher than 55N. It can also be stratified in coastal (35.7%) and land (64.3%) subset for other analysis.

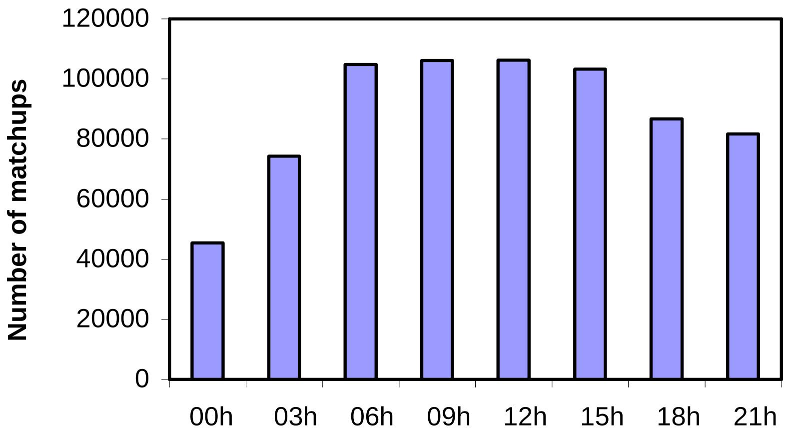

Figure 5 Frequency of 708793 SSD matchups according to their UTC observation hour.

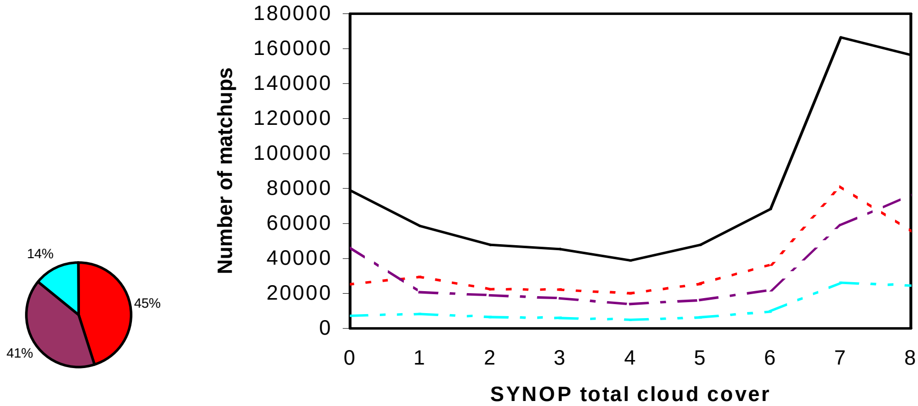

Figure 6 Left; SSD illumination conditions distribution; total (black), *day (red), night (purple), twilight (blue) Right; SSD frequency of matchups according to their total cloud cover in octas, globally and detailed by illumination condition; total (black solid line) , day (red dotted), night (purple dashed), twilight (blue dash-dotted).*

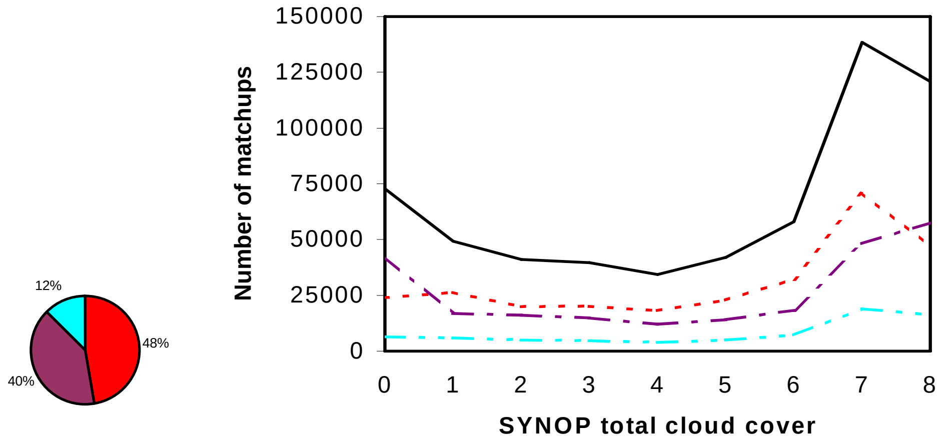

Figure 7 Same as figure above but for SSD midlatitude cases (total, *day*, *night*, *twilight*).

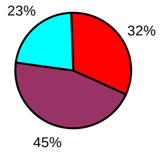

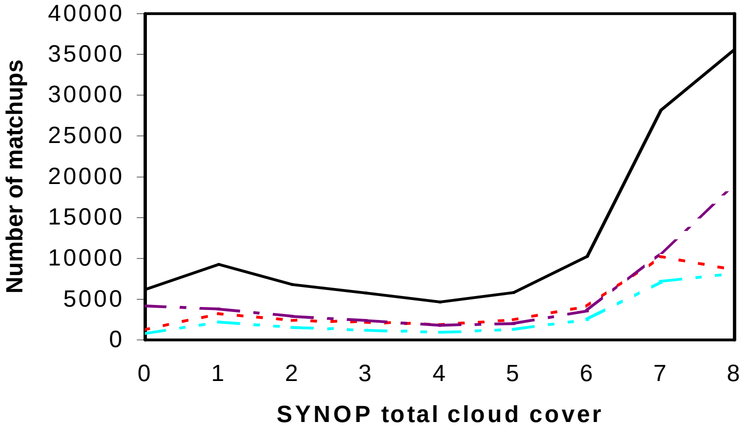

Figure 8 Same as figure above but for Nordic SSD cases (total, day, night, twilight).

The three figures above show that N1N7 anomaly is visible for daytime reports, that illumination distribution among dataset may vary. It is normal to see that geographical stratification changes slightly the illumination proportions, as twilight conditions become more numerous at northern latitudes.

ANNEX 4 GROUND-BASED RADAR AND LIDAR MEASUREMENTS AT SIRTA SITE (PARIS)

LIDAR instrument (LNA)

The lidar instrument, called Lidar Nuages Aerosols (LNA) is a backscattered lidar developed at LMD for cloud and aerosol remote sensing. It can detect aerosol and cloud layers with visible optical thickness ranging from 0.05 to 3, above which the signal is completely attenuated.

The LNA is an Nd-Yag pulsed lidar emitting at 532 and 1064 nm and linearly polarized. The pulse frequency is 20 Hz while the nominal temporal resolution is 10 s. Backscattered photons are collected through two telescopes: a narrow-field-of-view one (0.5 mrad) with range 2-15 km and a wide-field-of-view one (5 mrad) with range 0.1-5 km. The backscattered signal is sampled with a vertical resolution of 15 meters. Vertical distributions of particles are characterized from the ground to about 15 km and the structure of the atmosphere such as the boundary layer height and the altitudes of aerosol and cloud layer is derived by the STRAT algorithm (described below).

The LNA operates on routine schedules from Mondays through Fridays, 8am to 8pm local time. However, the LNA instrument is turned off in case of precipitation. Figure 9 shows the number of 15 min slots of LNA observation each month during the study period.

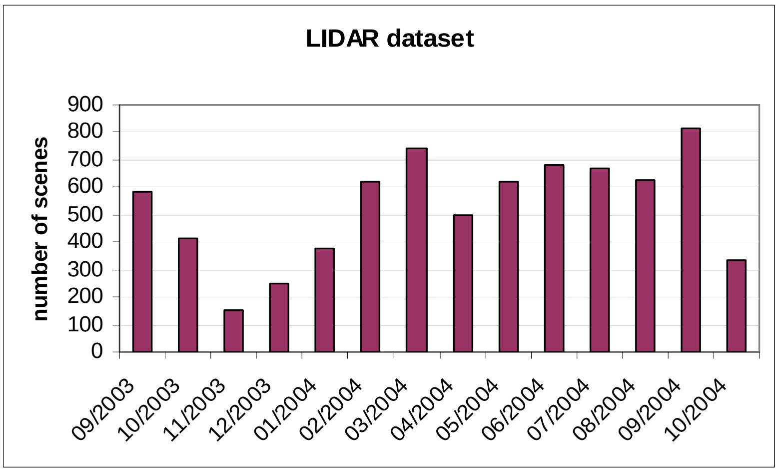

Figure 9 Distribution of LNA dataset (number of 15 min slots of observation each month).

Raw lidar data gives the amount of backscattered photons as a function of altitude for every profile. The LNA product used in this study is the output of the STRAT (STRucture of the ATmosphere) algorithm. It identifies the different layers crossed by the laser beam. In the v1 version of the STRAT algorithm, each pixel can be classified as:

- No significant power return (NSPR): the backscattered signal is considered too noisy for identification. A signal is considered too noisy when the signal to noise ratio is smaller than 3. The noise, caused by optical and electronic variations is considered constant along the profile. It is estimated by taking the standard deviation of the signal where there is no lidar return in the highest range (i.e. where the signal is totally due to sky radiance). The NSPR flag occurs in case the lidar beam is attenuated by the atmosphere underneath it.
- Boundary layer: the pixel is part of the boundary layer. It is the lowest layer of the atmosphere and is generally located between 1000 and 2000 meters altitude, depending on the intensity of the turbulent mixing (normally lower during night than during day). In this layer, where turbulence induced by the ground is very strong, the dynamics are different than in the higher layers. Most of the aerosols from the ground, mixed by turbulent flow,

are found inside this layer. In the STRAT algorithm, the boundary layer is identified by a threshold test applied on the ratio of the backscattering signal between two heights.

- Molecular: the atmosphere is cloud and aerosol free. A molecular backscattering profile is estimated from the comparison between pressure and temperature profiles (measured by daily atmospheric sounding or extracted from models) and the recording backscattered signal. Molecular layers correspond to zones that successfully passed a threshold test relevant of the similarity between the slopes of the simulated and measured profiles.
- Cloud or aerosol: the pixel is contaminated or filled by cloud or aerosol. Continuous Wavelet transform is used to detect singularities of the backscattering signal at layer boundaries (top, peak and base). A threshold test is also used to remove over detections due to noise fluctuations.
- Aerosol/cloud separation: based on the analysis of the particle backscatter distribution. A threshold on the average peak-to-base backscatter ratio of consistent particle layers is used to separate aerosol from cloud layers.

From this classification, a simplified cloud mask is derived as shown in Figure 10. The cloud mask reveals that the lidar provides a full characterization of the vertical extent of the cirrus cloud (07:00 to 12:00 UT), but as the cloud becomes optically thicker, the lidar signal is attenuated and the range is limited to the lowest 2 km of the cloud.

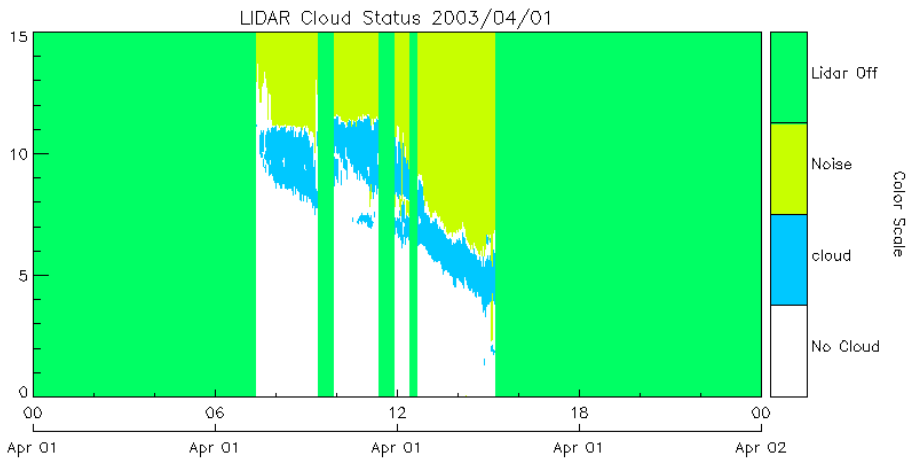

Figure 10 Cloud mask derived from the lidar backscattered power (green: lidar off, yellow: noise, blue: cloud, white: no cloud).

RADAR instrument (RASTA)

The cloud radar called RASTA (Radar Aéroporté et Sol de Télédétection Atmosphérique) is a vertically-pointing single beam 95GHz Doppler radar with a range resolution of 60 meters and the temporal resolution is 1 s. This instrument is devoted to the investigation of cloud processes, through the documentation of the microphysical, radiative and dynamical properties of all type of non-precipitating clouds.

The ground-based configuration of the RASTA cloud radar operates routinely at SIRTA since October 2002 until September 2004. RASTA ceased functioning in October 2004. Figure 11 shows the number of 15 min slots of RASTA observation each month during the study period.

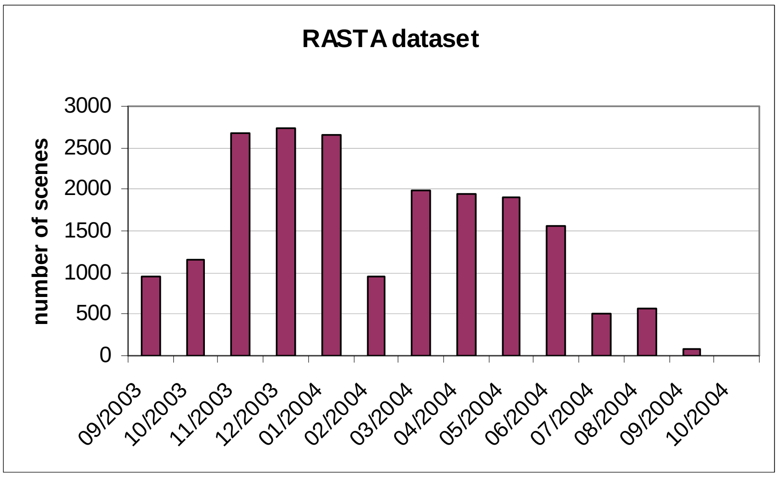

Figure 11 Distribution of RASTA dataset (number of 15 min slots of observation each month).

The radar products have been derived from an algorithm developed by the Department of Meteorology from the University of Reading (UK). This algorithm uses a multiple threshold tests on radar reflectivity and vertical Doppler velocity to classify pixels as : clear-sky, ice particles, melting ice particles, cloud liquid droplets, drizzle/rain, aerosols, or insects. We derive a simpler classification consisting of number 0 to 3 defined as :

0 : clear-sky, aerosol and insect pixels are deemed to be 'clear-sky'
1 : ice/water hydrometeor pixels are deemed to be 'cloud'
2 : precipitating hydrometeor pixels are deemed to be 'drizzle/rain'
3 : radar instrument turned off

Information of the retrieval algorithm can be found at http://www.met.rdg.ac.uk/radar/cloudnet/data/products/categorize.html.

Figure 12 shows the cloud mask derived from this algorithm.

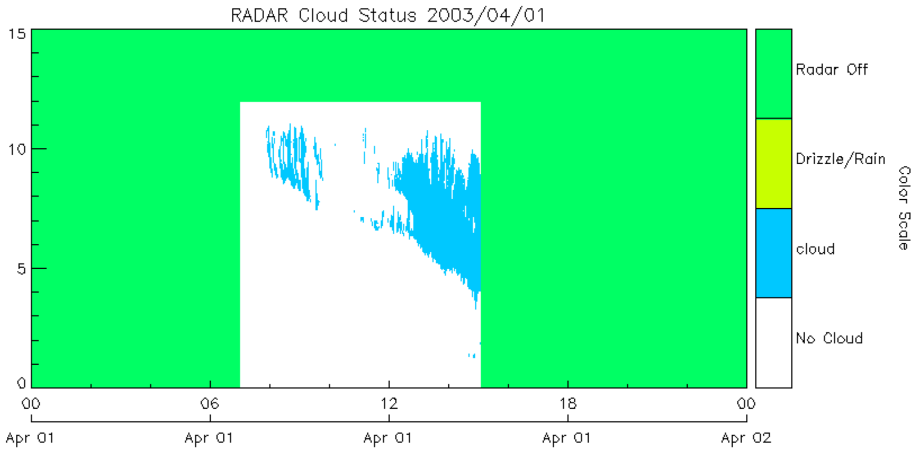

Figure 12 Cloud mask derived from the radar reflectivity (green: radar off, yellow: drizzle or rain, blue: cloud, white: no cloud)

Radar & Lidar synergy (RALI)

Data products retrieved from the synergy between the radar and lidar are called the RALI data in this study. The radar and lidar measurements are averaged over a 30 s timeframe and then are independently analysed to retrieve cloud mask product.

Figure 13 shows a cloud mask derived from the combined analysis of the radar reflectivity and the lidar backscattered power. Clouds shown in blue correspond to areas where one of the instruments detects clouds. The cloud mask reveals that radar-lidar synergy is particularly suited to extend the range of observable cloud layers. The vertical resolution is 60 m and the RALI measurements give a maximum range of 15 km.

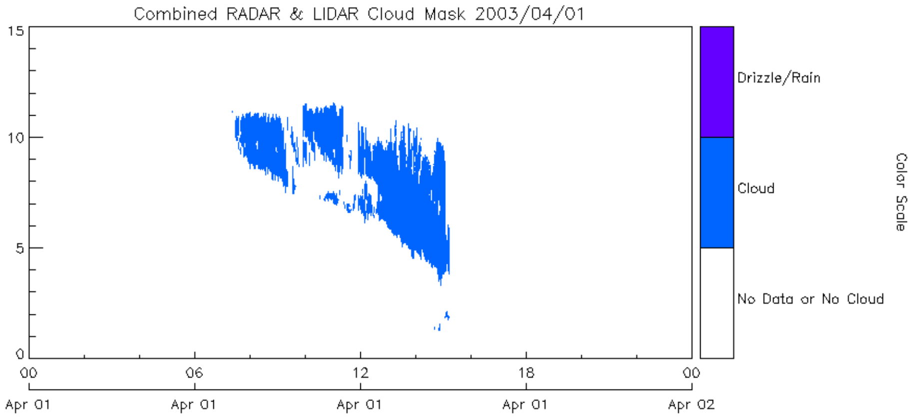

Figure 13 Cloud mask derived from radar-lidar synergy (violet: drizzle or rain, blue: cloud, white: no data or no cloud). The temporal resolution is 30 s.

RALI cloud mask datasets are available for 4 modes of measurement:

- Mode 0: measurement during radar data acquisition time
- Mode 1: measurement during simultaneous radar and lidar data acquisition time
- Mode 2: measurement during lidar data acquisition time
- Mode 3: measurement during radar and/or lidar data acquisition time

Remote sensing of clouds by lidar and radar : limitations

Active remote sensing by lidar only (mode 2):

Lidar back-scattering at 532 nm is sensitive to the number of scattering particles and second moment of the particle size distribution (D^2). The lidar beam is scattered by both liquid water and ice clouds. At each level of the atmosphere, scattering produces lidar signal (the back-scattered portion) but also lidar signal attenuation for the higher levels. For the LNA lidar we consider that the lidar signal is completely extinguished beyond an optical depth of about 3. We also consider that a cloud can be detected as long as its optical depth is greater than 0.01. According to Morille et al. (2005), for clouds with optical depth ranging between 0.01 and 3, the analysis of lidar back-scattered power by the STRAT algorithm will yield CTH values with a bias ranging from 0 to –60m (underestimation of CTH). In the following situations the lidar alone will not provide reliable CTH estimates for:

- Optically thick water clouds
- Ice clouds overlying a solid continuous layer of optically thick water clouds

Active remote sensing by radar only (mode 0):

Radar reflectivity at 94 GHz is driven by the number of particle and the sixth moment of the particle size distribution (D^6). The radar reflectivity is much more sensitive to particle size than particle concentration. Hence the radar will be efficient to detect clouds that contain a high amount of liquid or ice water in which cloud droplets and ice crystals have reached a significant size. Contrary to the lidar, the radar signal in clear air (outside the cloud) is virtually zero hence the cloud boundaries are easily found with a signal threshold. The only ambiguity is that if the cloud particles are too small or if the cloud is too thin and too far (> 10 km), the sensitivity of the radar is not sufficient to produce a reflectivity above the threshold. In the following situations the radar alone will not provide reliable CTH estimates for:

- Optically thin clouds above 10 km
- Fair weather cumulus clouds at the top of the boundary layer

Active remote sensing by lidar and radar (mode 1):

By combining the retrievals from lidar and radar observations, we are able to significantly decrease the number of clouds that are missed by the ground-based station. The combination of wavelengths allows us to observe the entire range of optical depth and cloud types. However, in the following situations the combination of lidar and radar at the ground may not be able to provide reliable CTH estimates for:

- Multi-layer situation with solid continuous layer of optically thick water clouds underlying a layer of optically thin ice clouds at a high altitude.

For all CTH validation studies, mode 1 is by far the most reliable data source, but the number of combined lidar/radar observation is smaller than lidar alone (mode 2) or radar alone (mode 0). Hence, to validate CTH values for:

- Opaque clouds, we use the mode 0 dataset.
- Semi-transparent clouds: we use the mode 2 dataset